

# Convergent Synthesis of a Metal–Organic Framework Supported Olefin Metathesis Catalyst

Jian Yuan,<sup>\*,†,‡,§</sup> Alejandro M. Fracaroli,<sup>†,‡</sup> and Walter G. Klemperer<sup>\*,‡,§</sup>

<sup>†</sup>Department of Chemistry, University of California, Berkeley, California 94720, United States

<sup>‡</sup>Materials Sciences Division, Lawrence Berkeley National Laboratory, Berkeley, California 94720, United States

<sup>§</sup>Department of Chemistry, University of Illinois at Urbana–Champaign, Urbana, Illinois 61801, United States

## Supporting Information

**ABSTRACT:** Synthesis of a metal–organic framework (MOF)-supported olefin metathesis catalyst has been accomplished for the first time following a new, convergent approach where an aldehyde-functionalized derivative of Hoveyda’s recently reported ruthenium catecholate olefin metathesis catalyst is condensed with an amine-functionalized IRMOF-74-III. The resulting material, denoted MOF-Ru, has well-defined, catalytically active ruthenium centers confined within channels having a ca. 20 Å diameter. MOF-Ru is a recyclable, single-site catalyst for self-cross-metathesis and ring-closing metathesis of terminal olefins. Comparison of this heterogeneous catalyst with a homogeneous analogue shows different responses to substrate size and shape suggestive of confinement effects. The MOF-Ru catalyst also displays greater resistance to double-bond migration that can be attributed to greater catalyst stability. For the preparation of well-defined, single-site heterogeneous catalysts where catalyst purity is essential, the convergent approach employed here, where the catalytic center is prepared ex situ and covalently linked to an intact MOF, offers an attractive alternative to in situ catalyst preparation as currently practiced in MOF chemistry.



## INTRODUCTION

The remarkably rapid development of metal–organic framework (MOF) catalysis in recent years can in no small part be attributed to advances in synthetic methodology allowing for the preparation of high-purity materials.<sup>1</sup> Catalyst purity has posed a serious challenge to the synthesis of single-site, metal-centered metal–organic framework catalysts since MOF catalysts, unlike their homogeneous analogues, cannot be purified using standard techniques such as distillation, recrystallization, chromatography, and sublimation.<sup>2</sup> The simplest approach to MOF catalysts, one-pot synthesis, has achieved great success,<sup>1,3</sup> but is restricted to those catalysts capable of withstanding the relatively harsh conditions associated with MOF synthesis. This limitation has been successfully circumvented in many instances by first preparing a MOF containing an appropriately reactive linker and then assembling an active catalyst in situ at this reactive site by postsynthetic modification.<sup>1,4</sup> This serial approach, which has traditionally found widespread application in oxide- and polymer-supported systems,<sup>5</sup> has dramatically expanded the domain of MOF catalysis. But it also has limitations for the preparation of well-defined, single-site MOF catalysts when aggressive reagents are required and side reactions occur in the course of catalyst preparation, since catalyst purification is not an option.<sup>6</sup>

Here we describe a new alternative to the one-pot and in situ postsynthetic approaches to MOF catalysts just described. A convergent approach is adopted where a metal-containing

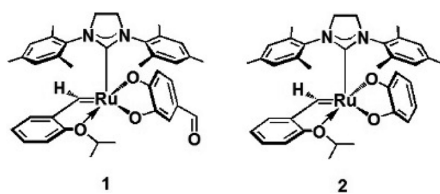
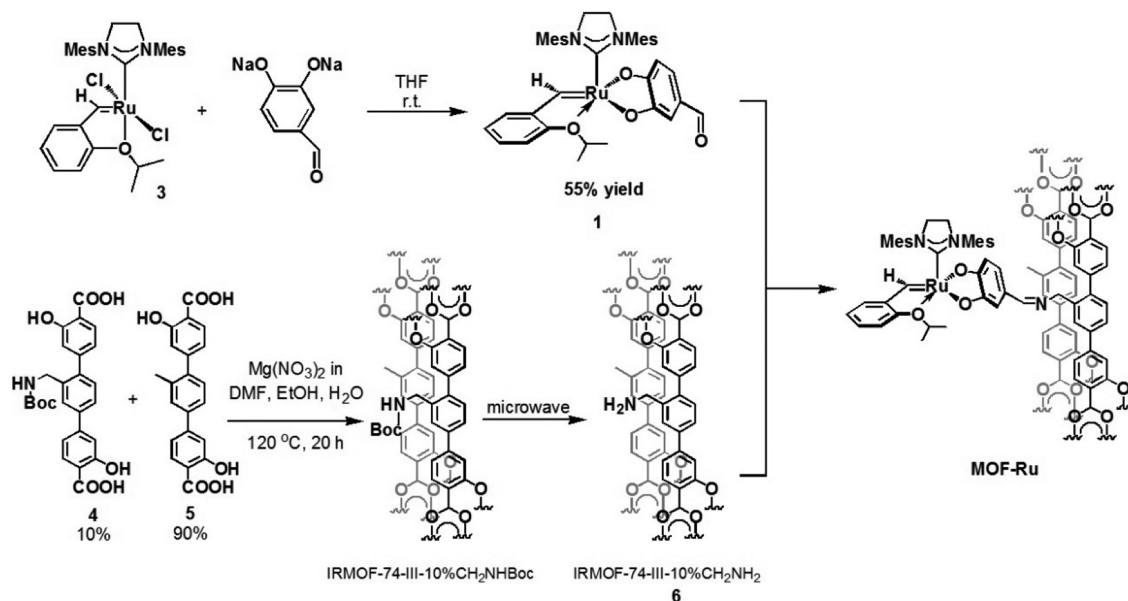
catalyst is prepared ex situ and then covalently attached to a MOF linker postsynthetically under mild reaction conditions where the catalyst is known to be stable and the MOF framework remains intact. Preparation of heterogeneous catalysts in this fashion by “tethering” has been investigated for Ru-based olefin metathesis catalysts on oxide and polymer supports,<sup>9,10</sup> since catalyst stability<sup>11</sup> and purity<sup>12</sup> are known to be critically important in the corresponding homogeneous systems. Catalyst–support interactions are believed to be important in oxide-supported ruthenium metathesis catalysts,<sup>10b,13</sup> but these interactions have been difficult to understand in detail due to the structurally ill-defined nature of the amorphous supports involved. In contrast, MOF supports are crystalline and structurally well-defined, and they offer the opportunity to tailor the environment of the catalytic center such that phenomena such as confinement effects might be engineered and tuned at will.

## RESULTS AND DISCUSSION

The strategy adopted here was to prepare the aldehyde-functionalized ruthenium catalyst **1** and the amine-functionalized MOF **6** independently (see Scheme 1) and then form the MOF-supported catalyst MOF-Ru by imine condensation under conditions where the ruthenium catalyst and the MOF are stable (see Scheme 1). Hoveyda’s catecholate complex<sup>14</sup> **2**

**Received:** May 5, 2016

Scheme 1



was selected for study since its catechol ligand could be functionalized, and once attached to a MOF, the catalytically active metal center would be confined between a bulky *N*-heterocyclic carbene ligand and the MOF surface. Amine-functionalized IRMOF-74-III<sup>15</sup> was selected due to its simple, one-dimensional, hexagonal channels defined by magnesium–oxygen chains and terphenylene linkers. Its ca. 20 Å pore diameter is wide enough to accommodate Hoveyda’s complex but narrow enough to provide a confined environment for the catalyst (see Figure 1). The hope was that confinement, although it would undoubtedly lead to slow substrate diffusion and hence low reaction rates, might lead to size or shape selectivity. However, the choice of a small pore diameter raised the possibility that binding of the catalyst to the MOF during MOF-Ru synthesis might block access of further catalyst molecules to the interior of the MOF. Active site isolation was achieved by preparing the mixed-linker MOF IRMOF-74-III-10%CH<sub>2</sub>NH<sub>2</sub> (6), where only 10% of the linkers were amine functionalized.<sup>16</sup> The air-sensitive ruthenium complex 1 was prepared from the Hoveyda–Grubbs Catalyst 2nd Generation<sup>17</sup> 3 following the procedure reported for the preparation of complex 2<sup>14</sup> but substituting 3,4-dihydroxybenzaldehyde for benzene-1,2-diol (see Scheme 1). Two isomers were obtained in a 2.7:1 ratio presumably corresponding to the two orientations possible for the catechol ligand in 1. According to a single-crystal X-ray diffraction study,<sup>18</sup> the ruthenium coordination geometry in 1 was very similar to that observed for 2 (Table S1.2). The MOF support 6 was prepared following the procedure reported for IRMOF-74-III-CH<sub>2</sub>NH<sub>2</sub><sup>15</sup> but replacing 90% of the *tert*-butyloxycarbonyl-protected aminomethyl linker 4 with its methyl analogue 5. Hoveyda has demonstrated the instability of his ruthenium catecholate catalyst toward protic reagents,<sup>18</sup> and in order to minimize the

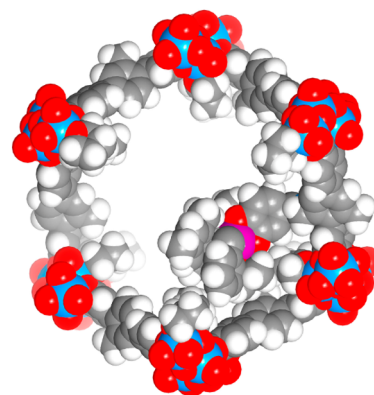


**Figure 1.** Structural diagram illustrating the relative sizes of the Ru complex 1 and the IRMOF-74-III channel in MOF-Ru after imine condensation with MOF 6. The diagram was generated from the crystallographic structure determinations of 1 (see text) and IRMOF-74-III.<sup>9</sup> Coordinated THF molecules and the imine linkage were then introduced, and energy was minimized using the Materials Studio Forcite molecular mechanics module. It represents only one of the many stable conformations and is intended only to show the relative sizes of 1 and the IRMOF-74-III channel. Oxygen atoms are colored red, magnesium colored blue, carbon colored gray, hydrogen colored white, and ruthenium colored violet.

presence of methanol and water in the MOF, the *N,N*-dimethylformamide (DMF) and methanol washing procedures were followed by tetrahydrofuran (THF) washings. There was some concern that the MOF-bound ruthenium catalyst might block access of unreacted ruthenium catalyst 1 to interior regions of the MOF channels (see Figure 1), and preparation of MOF-Ru was therefore carried out in two steps. First, activated 6 was suspended in a C<sub>6</sub>H<sub>6</sub> solution of 1 in a 1:0.1 mole ratio, and the suspension was stored in an argon atmosphere for 1 day in order to allow diffusion of 1 into 6. Activated molecular sieve desiccant was then added to the reaction mixture to promote the dehydration required for imine condensation; the color of the reaction solution changed from deep reddish-orange to light yellow as the reaction progressed. Other postsynthetic imine condensations have been performed in

Table 1. Metathesis of Olefins with MOF-Ru and 3

Entry	Substrate	MOF-Ru <sup>a</sup>			3 <sup>b</sup>		
		Product	yield (%) <sup>c</sup>	TON	Product	yield (%) <sup>c</sup>	TON
1		 C <sub>6</sub> H <sub>13</sub> –C <sub>6</sub> H <sub>13</sub>	71	142	 C <sub>6</sub> H <sub>13</sub> –C <sub>6</sub> H <sub>13</sub>	70 <sup>d</sup>	14
2			52	104		78	16
3			35	70		94 <sup>e</sup>	19
4			>99	>198		>99	20
5			26	52		76	15
6			3	6		77 <sup>f</sup>	15
			10	20	 and other olefins		

<sup>a</sup>0.5 mol % Ru catalyst in C<sub>6</sub>D<sub>6</sub> (0.146 M substrate) at room temperature for 72 h. <sup>b</sup>5 mol % Ru catalyst in C<sub>6</sub>D<sub>6</sub> (0.4 M substrate) at room temperature for 12 h. <sup>c</sup>Measured by <sup>1</sup>H NMR spectroscopy. <sup>d</sup>Small amounts of C<sub>9</sub>H<sub>18</sub>, C<sub>12</sub>H<sub>24</sub>, C<sub>13</sub>H<sub>26</sub>, and C<sub>15</sub>H<sub>30</sub> were formed (see Figure S19b). <sup>e</sup>Small amounts of CyCH=CH<sub>2</sub> and CyCH<sub>2</sub>CH=CHCy were formed (see Figure S21b). <sup>f</sup>Total yield of all the olefin products (see Figure S24b).

MOFs without the use of a dehydration agent,<sup>4b,19</sup> but one was required here most likely because amine groups in **6** could bind (reversibly) to the 16-electron metal center in **1**. This interpretation was supported by an HR-ESI-MS study of **1** in acetonitrile, which showed that an 18-electron acetonitrile adduct was formed (see Figure S3). Reaction of **1** with **6** was allowed to proceed for 3 days following addition of desiccant, and the reaction product isolated was formulated as Mg<sub>2</sub>L<sub>0.9</sub>L'<sub>0.06</sub>L''<sub>0.04</sub>(THF)<sub>1.5</sub>(H<sub>2</sub>O)<sub>0.5</sub> (L = unfunctionalized linker, L' = amine-functionalized linker, L'' = linker bound to the ruthenium catalyst). This formulation, derived from NMR and ICP-OES data presented in the Supporting Information, reflects a catalyst loading of about 40%, a value falling within the expected range.<sup>16</sup> Attempts to obtain spectroscopic support for the MOF-catalyst imine linkage were unsuccessful, presumably because of low catalyst loading, since only 4% of the linkers in the MOF were associated with catalytic centers. The color change observed upon reaction of the amine with the aldehyde and the failure to observe catalyst leaching (see below) leave little doubt that the desired linkage was in fact formed.

Initial efforts to prepare MOF-Ru yielded materials with only about 50% of the porosity exhibited by the IRMOF-74-III-10% CH<sub>2</sub>NH<sub>2</sub> starting material, **6**. This loss of porosity could be attributed to stirring of the reaction mixture with a magnetic stir bar, since (1) the porosity of **6** was maintained in the absence of stirring during the course of the MOF-Ru preparation and (2) stirring **6** in benzene for 4 days in the absence of **1** caused the same (~50%) reduction in porosity (see Figure S12).

MOF-Ru proved to be a viable olefin metathesis catalyst. Recycling experiments in C<sub>6</sub>D<sub>6</sub> using 100:1 substrate to ruthenium mole ratios and 1 day reaction times showed that styrene was converted into stilbene with only minimal reductions in yield as the catalyst was recycled. Successive yields of 71%, 69%, and 68% were observed, where the observed decrease in yields was most likely due to incomplete catalyst recovery since leaching of MOF-Ru yielded no soluble

catalyst. Details of these experiments are provided in the Experimental Section. Powder X-ray diffraction experiments showed no loss of MOF crystallinity after catalytic self-metathesis of 1-octene (Figure S11).

A series of self-cross-metathesis and ring-closing metathesis experiments were then performed to profile the catalytic activity of MOF-Ru in comparison with the commercially available Hoveyda–Grubbs Catalyst 2nd Generation<sup>17</sup> homogeneous catalyst, **3**. It was hoped that these comparative studies could utilize the precursor catalyst **1** rather than **3**, but this proved to be impractical since attempts to effect metathesis of 1-octene showed that **1** is a very poor metathesis catalyst, yielding over 10 major side products arising from double-bond migration (see Figure S25b). Benzene was selected as solvent since it minimized the double-bond migration observed in the homogeneous system.<sup>20</sup> First, conditions were established where similar reaction yields were observed for heterogeneous and homogeneous catalysis using 1-octene as a substrate. This was achieved using a 200:1 substrate to ruthenium ratio and a 72 h reaction time for the MOF-Ru heterogeneous catalyst and a 20:1 substrate to catalyst ratio and a 12 h reaction time for the homogeneous catalyst **3**, where both reactions proceeded in about 70% yield. The same experiments were then repeated using the terminal olefins styrene and allylcyclohexane and the  $\alpha$ - $\omega$  dienes 1,7-octadiene, 1,6-heptadiene, and 1,8-nondiene as substrates. The results of these experiments are shown in Table 1.

Note that for entries 1, 3, and 6 in Table 1 significant amounts of products were observed arising from olefin isomerization in the homogeneous case but not in the heterogeneous case. This reflects the greater stability expected for a supported catalyst, a result also observed in previous studies of supported ruthenium metathesis catalysts<sup>9</sup> and supported catalysts in general.<sup>5a,21</sup> Note also that the turnover numbers observed for the heterogeneous system are higher than those observed for the homogeneous system, reflecting the higher catalyst to substrate ratio reaction (200:1 vs 20:1) and

the longer reaction time (72 h vs 12 h) used in the heterogeneous case.

Results presented in Table 1 also provide evidence for confinement effects in the heterogeneous MOF-Ru catalyst. Comparison of entries 1–3 in Table 1, for example, shows that yields of homogeneous metathesis reactions increased slightly, but yields of the heterogeneous reactions dropped markedly as the steric bulk of the substrates was increased. Comparison of entries 4 and 6 shows unusually low 1,8-nonadiene conversion for the heterogeneous case relative to the homogeneous case. These trends could reflect slower diffusion of bulky substances from solution into the MOF pores,<sup>22</sup> slower diffusion through the MOF pores,<sup>22</sup> commensurate adsorption effects near the active site,<sup>23</sup> and/or slower metathesis in the confined environment of the catalytically active metal site. Distinguishing between these possibilities and exploiting their potential for shape-selective catalysis will require examination of substrates having a greater range of steric bulk and structural complexity.

## EXPERIMENTAL SECTION

**General Procedures.** All procedures were performed in an argon atmosphere using drybox or Schlenk techniques with the exception of thermogravimetric analysis (TGA) measurements. All glassware was oven-dried before use. Molecular sieves were activated at 200 °C for 24 h and then cooled to room temperature under vacuum. MOF digestion was achieved by suspending 10 mg of sample in 0.5 mL of DMSO-*d*<sub>6</sub> containing 10 μL of DCl in D<sub>2</sub>O (35 wt %), sonicating for about 1 min, and then allowing the suspension to stand at room temperature until a solution was obtained.

Sodium *tert*-butoxide, 3,4-dihydroxybenzaldehyde, Hoveyda–Grubbs Catalyst 2nd Generation, 35 wt % DCl in D<sub>2</sub>O (99 atom % D), and 3 Å molecular sieves were all purchased from Sigma-Aldrich and used as received. All of the olefin substrates were purchased from Sigma-Aldrich and dried with activated molecular sieves. Anhydrous THF, anhydrous CH<sub>2</sub>Cl<sub>2</sub>, anhydrous pentane, anhydrous acetonitrile, anhydrous toluene, and anhydrous diethyl ether were purchased from Sigma-Aldrich. Anhydrous DMF and methanol were obtained from EMD Millipore Chemicals. DMSO-*d*<sub>6</sub>, CDCl<sub>3</sub>, CD<sub>2</sub>Cl<sub>2</sub>, and C<sub>6</sub>D<sub>6</sub> were purchased from Cambridge Isotope Laboratories and dried over activated molecular sieves.

Proton NMR spectra were acquired on a Bruker Avance II spectrometer at 500 MHz. Chemical shifts were referenced to the deuterated solvents' residual proton resonances at 7.26 ppm for CDCl<sub>3</sub>, 7.16 ppm for C<sub>6</sub>D<sub>6</sub>, and 2.50 ppm for DMSO-*d*<sub>6</sub>. The following abbreviations are used below when describing resonances: s for singlet, d for doublet, sept for septet, and br for broad. High-resolution electrospray ionization mass spectra (HR-ESI-MS) were acquired on a Finnigan LTQ FT (Thermo Electron Corporation) instrument operating in positive ion mode by direct injection of the sample solution using syringe pump with a flow rate of 5 μL min<sup>-1</sup>. Powder X-ray diffraction (PXRD) patterns were measured using a Rigaku Miniflex 600 diffractometer (Bragg–Brentano geometry, Cu Kα radiation λ = 1.540 56 Å). Thermogravimetric analysis was performed on a TA Instruments Q500 analyzer. Nitrogen sorption isotherms were measured on a Quantachrome Autosorb-1 volumetric gas adsorption analyzer. Inductively coupled plasma-optical emission spectrometry (ICP-OES) was performed using an ICP Optima 7000 DV instrument. Gas chromatography–mass spectrometry (GC-MS) results were obtained using a Shimadzu GCMS-QP2010 SE instrument equipped with an SHRXI-SMS capillary column (30 m, 0.25 mm i.d., 0.25 μm film thickness). The carrier gas was helium (flow rate = 1 mL/min), and the detector voltage was 0.25 kV. Diluted samples (1.0 μL) were injected manually in split mode with the split ratio of 20.

**Disodium Salt of 3,4-Dihydroxybenzaldehyde (7).** This procedure is a slight modification of the procedure described in ref 14 for the preparation of the disodium salt of 1,2-dihydroxybenzene. A

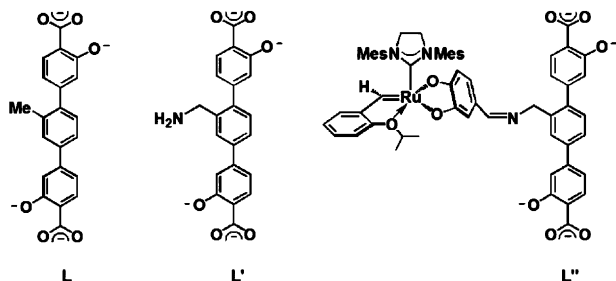
Schlenk flask was charged with 3,4-dihydroxybenzaldehyde (598 mg, 4.33 mmol), sodium *tert*-butoxide (1.00 mg, 10.4 mmol), and methanol (10 mL). This mixture was heated to 50 °C for 1 h with stirring. It was then cooled to room temperature, the solvent was removed under vacuum, and the residue was washed with 25 mL of THF. After drying for 12 h under vacuum, 731 mg (4.01 mmol) of product was obtained in 93% yield based on the 3,4-dihydroxybenzaldehyde starting material.

**Synthesis of Ruthenium Complex 1.** This procedure is a slight modification of the procedure described in ref 14 for the preparation of ruthenium complex 2. A solution of Hoveyda–Grubbs Catalyst 2nd Generation (100 mg, 0.16 mmol) in THF (2 mL) was added to a vial containing compound 7 (44 mg, 0.24 mmol). After the reaction solution had been stirred for 6 h at room temperature, the solvent was removed under vacuum, and the residue was purified as described in ref 14 for complex 2. Ruthenium complex 1 was obtained as a dark reddish-orange, microcrystalline solid (61 mg, 0.088 mmol, 55% yield based on Ru). HR-ESI-MS of CD<sub>3</sub>CN adduct in CH<sub>3</sub>CN solution (see Section S2): calcd for [M + H]<sup>+</sup>, [C<sub>40</sub>H<sub>43</sub>D<sub>3</sub>N<sub>3</sub>O<sub>4</sub>Ru]<sup>+</sup>, *m/z* = 737.2715; found *m/z* = 737.2728. Two isomers were obtained in a 2.7:1 ratio according to NMR spectral integrations (see Section S3). Major isomer, <sup>1</sup>H NMR (500 MHz, CD<sub>2</sub>Cl<sub>2</sub>, 22° C): δ 16.02 (s, Ru=CH, 1H), 9.48 (s, -CHO, 1H), 7.32 (ddd, <sup>3</sup>J<sub>av</sub> = 7.9 Hz, <sup>4</sup>J = 1.3 Hz, benzyldiene ligand aromatic CH, 1H), 7.06 (br s, mesityl aromatic CH, 2H), 7.00 (d, <sup>3</sup>J = 8.3 Hz, benzyldiene ligand aromatic CH, 1H), 6.91 (dd, <sup>3</sup>J = 7.7 Hz, <sup>4</sup>J = 1.6 Hz, catecholate ligand aromatic CH, 1H), ~6.9 (br s, mesityl aromatic CH, 1H), 6.88 (dd, <sup>3</sup>J<sub>av</sub> = 7.5 Hz, benzyldiene ligand aromatic CH, 1H), 6.82 (d, <sup>4</sup>J = 1.9 Hz, catecholate ligand aromatic CH, 1H), 6.736 (dd, <sup>3</sup>J = 8 Hz, <sup>4</sup>J = 2 Hz, benzyldiene ligand aromatic CH, 1H), 6.56 (d, <sup>4</sup>J = 8 Hz, catecholate ligand aromatic CH, 1H), 6.52 (br s, mesityl aromatic CH, 1H), 4.86 (sept, <sup>3</sup>J = 6.6 Hz, OCHMe<sub>2</sub>, 1H), 4.02 (s, NCH<sub>2</sub>CH<sub>2</sub>N, 4H), 2.48 (s, mesityl CH<sub>3</sub>, 6H), ~2.3 (br s, mesityl CH<sub>3</sub>, 3H), 2.25 (s, mesityl CH<sub>3</sub>, 6H), ~1.8 (br s, mesityl CH<sub>3</sub>, 3H), 1.47 (d, <sup>3</sup>J = 6.6 Hz, isopropyl CH<sub>3</sub>, 3H), 1.24 (d, <sup>3</sup>J = 6.3 Hz, isopropyl CH<sub>3</sub>, 3H). Minor isomer, <sup>1</sup>H NMR (500 MHz, CD<sub>2</sub>Cl<sub>2</sub>, 22° C): δ 16.32 (s, Ru=CH, 1H), 9.56 (s, -CHO, 1H), 7.32 (ddd, <sup>3</sup>J<sub>av</sub> = 7.9 Hz, <sup>4</sup>J = 1.3 Hz, benzyldiene ligand aromatic CH, 1H), 7.06 (br s, mesityl aromatic CH, 2H), 7.00 (d, <sup>3</sup>J = 8.3 Hz, benzyldiene ligand aromatic CH, 1H), 6.98 (d, <sup>4</sup>J = 2.1 Hz, catecholate ligand aromatic CH, 1H), ~6.9 (br s, mesityl aromatic CH, 1H), 6.89 (dd, <sup>3</sup>J<sub>av</sub> = 7.5 Hz, benzyldiene ligand aromatic CH, 1H), 6.79 (dd, <sup>3</sup>J = 8.1 Hz, <sup>4</sup>J = 2 Hz, catecholate ligand aromatic CH, 1H), 6.74 (dd, <sup>3</sup>J = 8 Hz, <sup>4</sup>J = 2 Hz, benzyldiene ligand aromatic CH, 1H), 6.52 (br s, mesityl aromatic CH, 1H), 6.42 (d, <sup>3</sup>J = 8 Hz, catecholate ligand aromatic CH, 1H), 4.81 (sept, <sup>3</sup>J = 6.4 Hz, OCHMe<sub>2</sub>, 1H), 4.02 (s, NCH<sub>2</sub>CH<sub>2</sub>N, 4H), 2.49 (s, mesityl CH<sub>3</sub>, 6H), ~2.3 (br s, mesityl CH<sub>3</sub>, 3H), 2.27 (s, mesityl CH<sub>3</sub>, 6H), ~1.8 (br s, mesityl CH<sub>3</sub>, 3H), 1.43 (d, <sup>3</sup>J = 6.6 Hz, isopropyl CH<sub>3</sub>, 3H), 1.22 (d, <sup>3</sup>J = 6.1 Hz, isopropyl CH<sub>3</sub>, 3H). Note that high concentrations of 1 lead to <sup>1</sup>H NMR line broadenings of the type observed for the analogous maleonitriledithiolate complex reported in ref 14. This most likely arises from intermolecular coordination of the catecholate ligand aldehyde oxygen atoms to ruthenium centers.

**Synthesis of IRMOF-74-III-10%CH<sub>2</sub>NH<sub>2</sub> (6).** This material was prepared following the same procedure used to prepare IRMOF-74-III-CH<sub>2</sub>NH<sub>2</sub> as described in ref 15a except that (a) 90% of linker 4 was replaced with linker 5 and (b) the DMF and methanol washing procedures were followed by washing with THF using the same protocol. The relative amounts of 4 and 5 actually incorporated into the MOF were determined from the <sup>1</sup>H NMR spectrum of the digested intermediate IRMOF-74-III-10%CH<sub>2</sub>NHBoc (see Figure S8), where the ratio of the intensity of the Boc methyl resonance in 4 to the intensity of the methyl resonance in 5 was 0.33, in good agreement with the 0.31 value calculated for a 1:9 molar ratio of 4 to 5. The nitrogen sorption isotherm of the reaction product is shown in Figure S12.

**Synthesis of MOF-Ru.** A deep reddish-orange solution of complex 1 (30 mg, 0.040 mmol) in C<sub>6</sub>D<sub>6</sub> (4 mL) was added to a suspension of 6 (200 mg, 0.38 mmol) in C<sub>6</sub>D<sub>6</sub> (4 mL). After 1 day, 15 pellets of activated molecular sieves were added to the reaction mixture, which

was swirled by hand three times a day for 3 days, causing a color change to light yellow. The solid material was isolated by filtration, washed with 5 mL of toluene, and then immersed in 10 mL of toluene. This toluene was removed by syringe and replaced with fresh toluene three times a day for 3 days. The solid product was then isolated by filtration, washed with 5 mL of toluene, and then dried under dynamic vacuum for 16 h to give 150 mg of a pale yellow solid. This material was characterized using TGA (Figure S10), PXRD (Figure S11), and nitrogen sorption porosimetry (Figure S12). It was formulated as  $Mg_{2.0}L_{0.9}L'_{0.06}L''_{0.04}(THF)_{1.5}(H_2O)_{0.5}$  using the  $L/(L' + L'')$  molar ratio determined for IRMOF-74-III-10%CH<sub>2</sub>NHBoc (see above and the following data). Ratio of the integrated intensity of CHO resonance to the integrated intensity of linker L CH<sub>3</sub> resonance in the <sup>1</sup>H NMR spectrum of digested sample (see Figure S9): calcd 0.015; found 0.013. Ratio of the integrated intensity of THF CH<sub>2</sub> resonance to the integrated intensity of the linker L CH<sub>3</sub> resonance in the <sup>1</sup>H spectrum of digested sample (see Figure S9): calcd 2.2; found 2.3. Three independently prepared samples were examined, and although PXRD, porosity, and NMR measurements were reproducible, TGA, CHN, and ICP-OES analyses were not reproducible within experimental error, presumably because activated MOF-Ru is a strong sorbent and absorbs varying amounts of volatiles from its drybox and atmospheric environment prior to CHN and TGA/ICP analyses, respectively. However, ICP-OES analysis reproducibly showed a Ru/Mg mole ratio of  $0.20 \pm 0.01$  (calcd 0.20).



**Heterogeneous Catalytic Olefin Metathesis.** A 4 mL vial was charged with MOF-Ru (5.0 mg, 9.2  $\mu$ mol, 0.37  $\mu$ mol of Ru), and 73  $\mu$ mol of substrate was added in 0.5 mL of C<sub>6</sub>D<sub>6</sub>, corresponding to 200:1 substrate to ruthenium molar ratio. After 3 days, a  $\sim$ 50  $\mu$ L aliquot was removed by pipet and diluted with CDCl<sub>3</sub> (0.5 mL) for NMR and GC-MS studies.

**Homogeneous Catalytic Olefin Metathesis.** A 4 mL vial was charged with olefin (0.20 mmol), and Hoveyda–Grubbs Catalyst 2nd Generation (6.2 mg, 0.010 mmol) was added to C<sub>6</sub>D<sub>6</sub> (0.5 mL) at room temperature, corresponding to a 20:1 substrate to ruthenium molar ratio. After 12 h, a  $\sim$ 50  $\mu$ L aliquot was removed by pipet and diluted with CDCl<sub>3</sub> (0.5 mL) for NMR and GC-MS studies. The same protocol and scale were used for the reaction of catalyst **1** with 1-octene.

**MOF-Ru Catalyst Recycling.** A 4 mL vial was charged with MOF-Ru (40 mg, 73  $\mu$ mol, 2.9  $\mu$ mol Ru), and a solution of styrene (30 mg, 0.29 mmol, 100 equiv per Ru) in C<sub>6</sub>D<sub>6</sub> (2 mL) was added. After 1 day, a  $\sim$ 50  $\mu$ L aliquot was removed by pipet and diluted with CDCl<sub>3</sub> (0.5 mL) for NMR analysis. The remaining MOF-Ru was then isolated by filtration, washed with C<sub>6</sub>D<sub>6</sub> (2 mL), and dried in vacuum. The procedure just described was then repeated two more times using the recycled MOF-Ru isolated from the reaction mixture in the previous cycle. According to <sup>1</sup>H NMR analysis, styrene was successively converted to stilbene in 71%, 69%, and 68% yield (see Figure S26).

**MOF-Ru Catalyst Leaching Experiments.** (1) A 4 mL vial was charged with MOF-Ru (2.5 mg, 4.6  $\mu$ mol, 0.19  $\mu$ mol of Ru) and 0.5 mL of CDCl<sub>3</sub>. After 1 day, the solid was filtered off and the colorless filtrate was charged with 50 mg of 1-octene. After 1 day, a  $\sim$ 10  $\mu$ L aliquot was removed by pipet and diluted with CDCl<sub>3</sub> (0.5 mL). No product was observed by <sup>1</sup>H NMR spectroscopy (see Figure S8.27). (2) A 4 mL vial was charged with MOF-Ru (40 mg, 73  $\mu$ mol, 2.9  $\mu$ mol of Ru), and a solution of styrene (30 mg, 0.29 mmol, 100 equiv per Ru) in C<sub>6</sub>D<sub>6</sub> (2 mL) was added. After 1 day, a  $\sim$ 50  $\mu$ L aliquot was

removed by pipet and diluted with CDCl<sub>3</sub> (0.5 mL) for NMR analysis (70% yield). The remaining solution was then separated from the catalyst by filtration. After 1 day, an aliquot of the solution was removed by pipet and diluted with CDCl<sub>3</sub> (0.5 mL) for NMR analysis (70% yield). According to <sup>1</sup>H NMR analysis, no further increase of yield was observed (see Figure S28).

## ■ ASSOCIATED CONTENT

### Supporting Information

The Supporting Information is available free of charge on the ACS Publications website at DOI: 10.1021/acs.organomet.6b00365.

Detailed synthetic procedures, HR-ESI mass spectra, <sup>1</sup>H NMR spectra, TGA traces, PXRD patterns, gas sorption isotherms, and NMR/GC-MS analysis of olefin metathesis product distributions (PDF)

Crystallographic data for the ruthenium complex **1** (CIF)

## ■ AUTHOR INFORMATION

### Corresponding Authors

\*E-mail (J. Yuan): jianyuanchem@gmail.com.

\*E-mail (W. G. Klemperer): wklemp@uiuc.edu.

### Present Address

◇ Quintara Biosciences, 170 Harbor Way, Suite 100, South San Francisco, California 94080, United States.

### Notes

The authors declare no competing financial interest.

## ■ ACKNOWLEDGMENTS

W.G.K. and J.Y. acknowledge Omar M. Yaghi, Felipe Gándara, Juncong Jiang, Yuebiao Zhang, Yingbo Zhao, Hiroyasu Furukawa, and Gregory Girolami for their invaluable advice and assistance. This research was funded by the U.S. Department of Defense, Defense Threat Reduction Agency (HDTRA 1-12-1-0053). Part of this research was performed at the Molecular Foundry as a user project, which was supported by the Office of Science, Office of Basic Energy Sciences, of the U.S. Department of Energy under Contract No. DE-AC02-05CH11231.

## ■ REFERENCES

- (1) For recent reviews see: (a) Garcia-Garcia, P.; Müller, M.; Corma, A. *Chem. Sci.* **2014**, *5*, 2979–3007. (b) Liu, J.; Chen, L.; Cui, H.; Zhang, J.; Zhang, L.; Su, C.-Y. *Chem. Soc. Rev.* **2014**, *43*, 6011–6061. (c) Gu, Z.-Y.; Park, J.; Raiff, A.; Wei, Z.; Zhou, H.-C. *ChemCatChem* **2014**, *6*, 67–75. (d) Zhao, M.; Ou, S.; Wu, C. D. *Acc. Chem. Res.* **2014**, *47*, 1199–1207. (e) Mondloch, J. E.; Farha, O. K.; Hupp, J. T. In *Metal Organic Frameworks as Heterogeneous Catalysts*; Llabrés i Xamena, F. X.; Gascon, J., Eds.; RSC Catalysis Series, No. 12; Royal Society of Chemistry: London, 2013; pp 289–309. (f) Llabrés i Xamena, F. X.; Luz, I.; Cirujano, F. G. In *Metal Organic Frameworks as Heterogeneous Catalysts*; Llabrés i Xamena, F. X.; Gascon, J., Eds.; RSC Catalysis Series, No. 12; Royal Society of Chemistry: London, 2013; pp 237–267. (g) Furukawa, H.; Cordova, K. E.; O’Keefe, M.; Yaghi, O. M. *Science (Washington, DC, U. S.)* **2013**, *341*, 1230444. (h) Wang, C.; Liu, D.; Lin, W. *J. Am. Chem. Soc.* **2013**, *135*, 13222–13234. (i) Dhakshinamoorthy, A.; Opanasenko, M.; Čejka, J.; Garcia, H. *Catal. Sci. Technol.* **2013**, *3*, 2509–2540. (j) Valvickens, P.; Vermoortele, F.; De Vos, D. *Catal. Sci. Technol.* **2013**, *3*, 1435–1445. (k) Yoon, M.; Srirambalaji, R.; Kim, K. *Chem. Rev.* **2012**, *112*, 1196–1231. (l) Canivet, J.; Farrusseng, D. *ChemCatChem* **2011**, *3*, 823–826. (m) Corma, A.; Garcia, H.; Llabrés i Xamena, F. X. *Chem. Rev.* **2010**, *110*, 4606–4655. (n) Farrusseng, D.; Aguado, S.; Pinel, C. *Angew. Chem., Int. Ed.* **2009**, *48*, 7502–7513. (o) Hong, D.-Y.; Hwang,

- Y. K.; Serre, C.; Férey, G.; Chang, J.-S. *Adv. Funct. Mater.* **2009**, *19*, 1537–1552.
- (2) Farha, O. K.; Mulfort, K. L.; Thorsness, A. M.; Hupp, J. T. *J. Am. Chem. Soc.* **2008**, *130*, 8598–8599.
- (3) For representative publications, see: (a) Wang, C.; Liu, D.; Xie, Z.; Lin, W. *Inorg. Chem.* **2014**, *53*, 1331–1338. (b) Mlinar, A. N.; Keitz, B. K.; Gygi, D.; Bloch, E. D.; Long, J. R.; Bell, A. T. *ACS Catal.* **2014**, *4*, 717–721. (c) Falkowski, J. M.; Liu, S.; Wang, C.; Lin, W. *Chem. Commun.* **2012**, *48*, 6508–6510. (d) Zhang, T.; Song, F.; Lin, W. *Chem. Commun.* **2012**, *48*, 8766–8768. (e) Wang, C.; Xie, Z.; deKrafft, K. E.; Lin, W. *J. Am. Chem. Soc.* **2011**, *133*, 13445–13454. (f) Song, F.; Wang, C.; Lin, W. *Chem. Commun.* **2011**, *47*, 8256–8258. (g) Phan, A.; Czaja, A. U.; Gándara, F.; Knobler, C. B.; Yaghi, O. M. *Inorg. Chem.* **2011**, *50*, 7388–7390. (h) Song, F.; Wang, C.; Falkowski, J. M.; Ma, L.; Lin, W. *J. Am. Chem. Soc.* **2010**, *132*, 15390–15398. (i) Hwang, Y. K.; Hong, D.-Y.; Chang, J.-S.; Seo, H.; Yoon, M.; Kim, J.; Jhung, S. H.; Serre, C.; Férey, G. *Appl. Catal., A* **2009**, *358*, 249–253. (j) Cho, S.-Y.; Ma, B.; Nguyen, S. T.; Hupp, J. T.; Albrecht-Schmitt, T. E. *Chem. Commun.* **2006**, 2563–2565.
- (4) For representative publications see: (a) Manna, K.; Zhang, T.; Greene, F. X.; Lin, W. *J. Am. Chem. Soc.* **2015**, *137*, 2665–2673. (b) Manna, K.; Zhang, T.; Carboni, M.; Abney, C. W.; Lin, W. *J. Am. Chem. Soc.* **2014**, *136*, 13182–13185. (c) Nguyen, H. G. T.; Schweitzer, N. M.; Chang, C.-Y.; Drake, T. L.; So, M. C.; Stair, P. C.; Farha, O. K.; Hupp, J. T.; Nguyen, S. T. *ACS Catal.* **2014**, *4*, 2496–2500. (d) Canivet, J.; Aguado, S.; Schuurman, Y.; Farrusseng, D. *J. Am. Chem. Soc.* **2013**, *135*, 4195–4198. (e) Nguyen, H. G. T.; Weston, M. H.; Sarjeant, A. A.; Gardner, D. M.; An, Z.; Carmieli, R.; Wasielewski, M. R.; Farha, O. K.; Hupp, J. T.; Nguyen, S. T. *Cryst. Growth Des.* **2013**, *13*, 3528–3534. (f) Wang, C.; Wang, J. L.; Lin, W. *J. Am. Chem. Soc.* **2012**, *134*, 19895–19908. (g) Bhattacharjee, S.; Yang, D.-A.; Ahn, W.-S. *Chem. Commun.* **2011**, *47*, 3637–3639. (h) Ingleson, M. J.; Barrio, J. P.; Guilbaud, J.-B.; Khimyak, Y. Z.; Rosseinsky, M. J. *Chem. Commun.* **2008**, 2680–2682.
- (5) (a) Hartley, F. R. *Supported Metal Complexes*; Reidel Publishing: Dordrecht, 1985. (b) Copéret, C.; Comas-Vives, A.; Conley, M. P.; Estes, D. P.; Fedorov, A.; Mougél, V.; Nagae, H.; Núñez-Zarur, F.; Zhizhko, P. A. *Chem. Rev.* **2016**, *116*, 323–421. (c) For an overview of postpolymerization modification see: Günay, K. A.; Theato, P.; Klok, H.-A. In *Functional Polymers by Post-Polymerization Modification: Concepts, Guidelines, and Applications*; Theato, P., Klock, H.-A., Eds.; Wiley-VCH: Weinheim, 2013; pp 1–44.
- (6) Consider, for example, the remarkably reactive and selective asymmetric catalysts obtained by postsynthetic metalation of MOF linkers derived from 1,1'-bi-2-naphthol (BINOL) using  $\text{Ti}(\text{O}^i\text{Pr})_4$ .<sup>7a</sup> Here, a titanium loading measurement was reported, revealing that at most 68 mol % of the titanium present could be assigned to the desired  $\text{Ti}(\text{BINOL})$  catalyst, with a least 32 mol % arising from undesired side reactions. In a related  $\text{Ti}(\text{BINOL})$  catalyst,<sup>7b</sup> at least 40 mol % of the titanium present arose from side reactions. The side reactions presumably arose from titanium alkoxide hydrolysis/condensation: in both cases the MOF precursors contained far more water than BINOL groups, and  $\text{Ti}(\text{O}^i\text{Pr})_4$  is extremely moisture sensitive, forming polytitanates upon exposure to water.<sup>8</sup>
- (7) (a) Ma, L.; Falkowski, J. M.; Abney, C.; Lin, W. *Nat. Chem.* **2010**, *2*, 838–846. (b) Ma, L.; Wu, C. D.; Wanderley, M. M.; Lin, W. *Angew. Chem., Int. Ed.* **2010**, *49*, 8244–8248.
- (8) (a) Bradley, D. C.; Mehrotra, R. C.; Rothwell, I. P.; Singh, A. *Alkoxo and Aryloxo Derivatives of Metals*; Academic Press: San Diego, 2001; p 108. (b) Turova, N. Ya.; Turevskaya, E. P.; Kessler, V. G.; Yanovskaya, M. I. *The Chemistry of Metal Alkoxides*; Kluwer: Dordrecht, 2002; p 121.
- (9) For recent reviews see: (a) Allen, D. P. In *Handbook of Metathesis Vol. 1: Catalyst Development and Mechanism*, 2nd ed.; Grubbs, R. H., Wenzel, A. G., Eds.; Wiley-VCH: Weinheim, 2015; pp 97–158. (b) Buchmeister, M. R. In *Olefin Metathesis: Theory and Practice*; Grela, K., Ed.; Wiley: New York, 2014; pp 495–514. (c) Hamad, F. B.; Kai, C.; Cai, Y.; Xie, Y.; Lu, Y.; Ding, F.; Sun, Y.; Verpoort, F. *Curr. Org. Chem.* **2013**, *17*, 2592–2608. (d) Balcar, H.; Čejka, J. *Coord. Chem. Rev.* **2013**, *257*, 3107–3124. (e) Copéret, C.; Basset, J.-M. *Adv. Synth. Catal.* **2007**, *349*, 78–92.
- (10) For representative publications see: (a) Monge-Marcet, A.; Pleixats, R.; Cattoën, X.; Man, M. W. C. *Tetrahedron* **2013**, *69*, 341–348. (b) Allen, D. P.; Van Wingerden, M. M.; Grubbs, R. H. *Org. Lett.* **2009**, *11*, 1261–1264. (c) Li, L.; Shi, J. *Adv. Synth. Catal.* **2005**, *347*, 1745–1749. (d) Mayr, M.; Wang, D.; Kröll, R.; Schuler, N.; Prühs, S.; Fürstner, A.; Buchmeiser, M. R. *Adv. Synth. Catal.* **2005**, *347*, 484–492. (e) De Clercq, B.; Lefebvre, F.; Verpoort, F. *Appl. Catal., A* **2003**, *247*, 345–364.
- (11) Schrodri, Y. In *Handbook of Metathesis Vol. 1: Catalyst Development and Mechanism*, 2nd ed.; Grubbs, R. H., Wenzel, A. G., Eds.; Wiley-VCH: Weinheim, 2015; pp 323–342.
- (12) (a) Sutton, A. E.; Seigel, B. A.; Finnegan, D. F.; Snapper, M. L. *J. Am. Chem. Soc.* **2002**, *124*, 13390–13391. (b) Hekking, K. F. W.; van Delft, F. L.; Rutjes, F. P. J. T. *Tetrahedron* **2003**, *59*, 6751–6758. (c) van Lierop, B. J.; Reckling, A. M.; Lummiss, J. A. M.; Fogg, D. E. *ChemCatChem* **2012**, *4*, 2020–2025.
- (13) Samantaray, M. K.; Alauzun, J.; Gajan, G.; Kavitate, S.; Mehdi, A.; Veyre, L.; Lelli, M.; Lesage, A.; Emsley, L.; Copéret, C.; Thieuleux, C. *J. Am. Chem. Soc.* **2013**, *135*, 3193–3199.
- (14) Khan, R. K. M.; Torker, S.; Hoveyda, A. H. *J. Am. Chem. Soc.* **2013**, *135*, 10258–10261.
- (15) (a) Fracaroli, A. M.; Furukawa, H.; Suzuki, M.; Dodd, M.; Okajima, S.; Gándara, F.; Reimer, J. A.; Yaghi, O. M. *J. Am. Chem. Soc.* **2014**, *136*, 8863–8866. (b) Deng, H.; Grunder, S.; Cordova, K. E.; Valente, C.; Furukawa, H.; Hmadeh, M.; Gándara, F.; Whalley, A. C.; Liu, Z.; Asahina, S.; Kazumore, H.; O'Keefe, M.; Terasaki, O.; Stoddart, J. F.; Yaghi, O. M. *Science (Washington, DC, U. S.)* **2012**, *336*, 1018–1023.
- (16) Mixed ligand compositions designed to enforce catalyst site isolation and likely catalyst loadings were estimated as follows. The channel diameter in the IRMOF-74-III structure is about 20 Å, and the tethered catalyst extends about 10 Å into the channel, as shown in Figure 1. Layers of linkers lining the channels in this structure are separated by 6.5 Å, and the thickness of the tethered catalyst measured along the channel axis is about 13 Å. Nearest neighbor contacts between tethered catalysts can in principal be avoided if each catalyst “blocks” access to all other linkers in the same layer and all linkers in the two adjacent layers. In this case, only 1/9 (11%) of the linkers could bear amine groups in a perfectly ordered structure. However, the mixed linker structure is almost certainly not ordered, and shorter separations between neighboring functionalized linkers will almost certainly occur. Consider the present case where only 10% of the linkers are functionalized. In a completely disordered structure, two types of disorder can occur. First, there is a 10% probability that each of the  $6 + 5 + 6 = 17$  nearest neighbor linkers to each amine-functionalized linker will be another amine-functionalized linker. Second, there is a 50% chance that each amine-functionalized phenylene groups will occupy one of the two possible rotameric configurations. This means that there is still a  $(1/10)(17)(1/2) = 17/20$  (85%) probability of a “blocked” site being occupied by another amine-functionalized ligand and only a 3/20 (15%) probability that a “blocked” site will not be occupied.
- (17) (a) Garber, S. B.; Kingsbury, J. S.; Gray, B. L.; Hoveyda, A. H. *J. Am. Chem. Soc.* **2000**, *122*, 8168–8179. (b) Gessler, S.; Randl, S.; Blechert, S. *Tetrahedron Lett.* **2000**, *41*, 9973–9976.
- (18) Kahn, R. K. M.; Torker, S.; Hoveyda, A. H. *J. Am. Chem. Soc.* **2014**, *136*, 14337–14340.
- (19) Doonan, C. J.; Morris, W.; Furukawa, H.; Yaghi, O. M. *J. Am. Chem. Soc.* **2009**, *131*, 9492–9493.
- (20) (a) Hanson, P. R.; Maitra, S.; Chegondi, R.; Markley, J. L. In *Handbook of Metathesis Vol. 2: Applications in Organic Synthesis*, 2nd ed.; Grubbs, R. H., O'Leary, D. J., Eds.; Wiley-VCH: Weinheim, 2015; pp 1–170. (b) Nam, Y. H.; Snapper, M. L. In *Handbook of Metathesis Vol. 2: Applications in Organic Synthesis*, 2nd ed.; Grubbs, R. H., O'Leary, D. J., Eds.; Wiley-VCH: Weinheim, 2015; pp 311–380. (c) van Lierop, B. J.; Lummiss, J. A. M.; Fogg, D. E. In *Olefin Metathesis: Theory and Practice*; Grela, K., Ed.; Wiley: New York, 2014;

pp 85–152. (d) Żukowska, K.; Grela, K. In *Olefin Metathesis: Theory and Practice*; Grela, K., Ed.; Wiley: New York, 2014; pp 39–83.

(21) Yermakov, Yu. I.; Kuznetsov, B. N.; Zakharov, V. A. *Catalysis by Supported Complexes*; Elsevier: Amsterdam, 1981.

(22) (a) Tzoulaki, D.; Heinki, L.; Lim, H.; Li, J.; Olson, D.; Caro, J.; Krishna, R.; Chmelik, C.; Kärger, J. *Angew. Chem., Int. Ed.* **2009**, *48*, 3525–3528. (b) Hibbe, F.; Chmelik, C.; Heinke, L.; Pramanik, S.; Li, J.; Ruthven, D. M.; Tzoulaki, D.; Kärger, J. *J. Am. Chem. Soc.* **2011**, *133*, 2804–2807.

(23) Wu, H.; Gong, Q.; Olson, D. H.; Li, J. *Chem. Rev.* **2012**, *112*, 836–868.